

Development and Validation of a Dynamic Kidney Failure Prediction Model based on Deep Learning: A Real-World Study with External Validation

Jingying Ma^{a,b,1}, Jinwei Wang^{c,d,e,1}, Lanlan Lu^f, Yexiang Sun^g, Mengling Feng^{b,h}, Peng Shen^g, Zhiqin Jiang^{g,*}, Shenda Hong^{a,i,*}, Luxia Zhang^{a,c,d,e,*}

^aNational Institute of Health Data Science, Peking University, 38 Xueyuan Road, Haidian District, Beijing, 100191, Beijing, China

^bSaw Swee Hock School of Public Health, National University of Singapore, 12 Science Drive 2, Singapore, 117549, Singapore, Singapore

^cRenal Division, Department of Medicine, Peking University First Hospital, No.8 Xishiku Street, Xicheng District, Beijing, 100034, Beijing, China

^dResearch Units of Diagnosis and Treatment of Immune-Mediated Kidney Diseases, Chinese Academy of Medical Sciences, No.9 Dongdan Santiao, Dongcheng District, Beijing, 100730, Beijing, China

^eState Key Laboratory of Vascular Homeostasis and Remodeling, Peking University, 38 Xueyuan Road, Haidian District, Beijing, 100191, Beijing, China

^fXiaying primary health care center, Ningbo Yinzhou No.2 Hospital, No.1092 Qianhe North Road, Ningbo, 315192, Zhejiang province, China

^gYinzhou District Center for Disease Control and Prevention, No.1221 Xueshi Road, Ningbo, 315040, Zhejiang province, China

^hInstitute of Data Science, National University of Singapore, 3 Research Link, Singapore, 117602, Singapore, Singapore

ⁱNHC Key Laboratory of Cardiovascular Molecular Biology and Regulatory Peptides, Peking University, 38 Xueyuan Road, Haidian District, Beijing, 100191, Beijing, China

Abstract

Background. Chronic kidney disease (CKD), a progressive disease with high morbidity and mortality, has become a significant global public health problem. At present, most of the models used for predicting the progression of CKD are static models. We aim to develop a dynamic kidney failure prediction model based on deep learning (KFDeep) for CKD patients, utilizing all available data on common clinical indicators from real-world Electronic Health Records (EHRs) to provide real-time predictions.

Methods. We use eight variables as predictors, including two demographic factors (age and gender) and six repeated common clinical indicators (estimated glomerular filtration rate (eGFR), urine albumin-to-creatinine ratio (uACR), albumin levels, blood calcium, blood phosphorus, and bicarbonate (HCO₃) levels). To leverage all historical data on these indicators to dynamically predict the progression to kidney failure in individuals with CKD stages 3 to 5, we use time-aware long short-term memory framework, a deep learning approach, to build the model. We assess the model's performance by calculating the area under the receiver operating

*Corresponding Authors.

Email addresses: 2210221440@qq.com (Zhiqin Jiang), hongshenda@pku.edu.cn (Shenda Hong), zhanglx@bjmu.edu.cn (Luxia Zhang)

¹Co-first Authors.

characteristic curve (AUROC) with a 95% confidence interval (CI). Furthermore, we conduct subgroup analyses, interpret the model using SHapley Additive exPlanations (SHAP), and validate the alignment between the clustering results of the neural network’s hidden layers and established medical knowledge. Additionally, we explicitly extract the model weights and transform them into a set of visible equations. Consequently, the model becomes fully interpretable and is not dependent on any specific deep learning architecture. We deploy the model on an open-source website to facilitate easy access and use.

Findings. A retrospective cohort of 4,587 patients from EHRs of Yinzhou, China, is used as the development dataset (2,752 patients for training, 917 patients for validation) and internal validation dataset (917 patients), while a prospective cohort of 934 patients from the Peking University First Hospital CKD cohort (PKUFH cohort) is used as the external validation dataset. The AUROC of the KFDeep model reaches 0.946 (95% CI: 0.922-0.970) on the internal validation dataset and 0.805 (95% CI: 0.763-0.847) on the external validation dataset, both surpassing existing models. The KFDeep model demonstrates stable performance in simulated dynamic scenarios, with the AUROC progressively increasing over time. Both the calibration curve and decision curve analyses confirm that the model is unbiased and safe for practical use, while the SHAP analysis and hidden layer clustering results align with established medical knowledge.

Interpretation. The KFDeep model built from real-world EHRs enhances the prediction accuracy of kidney failure without increasing clinical examination costs and can be easily integrated into existing hospital systems, providing physicians with a continuously updated decision-support tool due to its dynamic design.

Funding. National Natural Science Foundation of China.

Keywords: Chronic Kidney Disease, Kidney Failure, Electronic Health Record, Dynamic Deep Learning Model

1. Introduction

Chronic kidney disease (CKD) is an important public health problem with a prevalence of 10%-16% in major countries and with a rising trend of mortality, which is projected to become the 5th leading cause of death in 2040 [1, 2]. Besides, some patients will eventually progress to kidney failure, requiring lifelong dialysis or kidney transplantation to maintain survival. The therapies also lead to substantially reduced quality of life and increased medical expenses [3, 4]. Since CKD is asymptomatic in early stages while incurable when reaching moderate to advanced stages, early diagnosis and timely treatment for patients with CKD are of paramount importance [5].

Prediction models play a crucial role in forecasting the progression of chronic kidney disease (CKD) and guiding optimal management strategies. Among these, the Kidney Failure Risk Equations (KFREs) are the most well-validated across diverse populations worldwide [6, 7]. The simple form of KFREs includes age, sex, estimated glomerular filtration rate (eGFR), and urine albumin, while the extended ones add four serum laboratory measures. Although AI models can handle complex interactions and collinearity among variables, existing machine learning models have shown limited improvement over KFREs in practice [8]. Therefore, there

is a need for deep learning models that can better capture complex patterns and automatically learn from large datasets.

Moreover, research has shown that repeated measurements of indicators, such as eGFR, significantly improve the precision of prediction models for the progression of CKD [9]. However, most of the existing models are static, relying on single time step data and missing the benefits of tracking changes over time [6, 7]. Deep learning models, particularly recurrent neural networks like Long Short-Term Memory (LSTM) models [10], have a clear advantage in capturing temporal patterns, making them well suited for modeling repeated measurements in longitudinal health data. Although these models have achieved success in various medical applications [11, 12], they are still rarely applied to kidney failure prediction. This underscores the need for dynamic deep learning models that can fully utilize longitudinal data to provide more accurate and clinically relevant kidney failure predictions.

Therefore, we develop a dynamic kidney failure risk prediction model, which considers repeatedly measured common clinical indicators of CKD and can provide real-time diagnosis, called time-aware dynamic kidney failure prediction model (KFDeep). Model bias is assessed by calibration curve, decision curve analysis and subgroup analysis. We use SHAP analysis and hidden layer clustering to analyze the interpretability of the model in detail. Additionally, we created a web-based calculator to showcase our model: <https://visdata.bjmu.edu.cn/kfdeep>. The code is available at <https://github.com/PKUDigitalHealth/KFDeep>.

2. Methods

This study aims to develop a dynamic prediction model for kidney failure using the same predictors involved in KFREs. The study can be divided into 4 steps: model development, evaluation, robustness analysis, and interpretation. First, we developed the prediction model based on the CK-NET-Yinzhou cohort, an electronic health records (EHR) based cohort from a coastal city in east China [13]. Second, internal, temporal, and external validations (based on another hospital-based cohort) were conducted. Model calibration and decision curve analysis were also performed. Third, we performed subgroup analyses based on gender and age. Fourth, we used the SHAP model and clustered the deep features with dimension reduction for visualization. The study was performed and reported according to the TRIPOD guideline [14].

2.1. Study Population

The study has two source populations. For model development and internal validation, we use a retrospective cohort, CK-NET-Yinzhou study, which is a real-world EHR-based cohort involving permanent residents registered in the Regional Health Information System of Yinzhou district in Ningbo City, Zhejiang province, China. The Yinzhou Health Information System integrates various data streams, including public health management, health examination, outpatient visits and hospitalizations [15]. From 2018, a local registry of CKD has been established by extracting data based on specific International Classification of Diseases (ICD) codes and abnormalities in lab tests [16]. Between 1st May, 2008 and 31st Dec, 2019, we identified 85,519 patients with CKD from a total of 976,409 individuals registered in the database [17]. In the current study, to fulfill the requirement of chronicity in the definition of CKD and keep aligned with that used in the original KFREs study, we involved only patients with $eGFR \leq 60ml/min/1.73m^2$ for ≥ 2 times separated by a period of ≥ 3 months to ≤ 2 years as the study sample. The date for the second $eGFR \leq 60ml/min/1.73m^2$ is assigned as

the index date. In addition, we excluded patients who had already been under maintenance dialysis treatment on the index date or who initiated dialysis within 3 months after the index date (due to the high possibility of having already entered kidney failure before the index date). The study received approval from the Institutional Review Board at Peking University First Hospital (Approval ID: 2019[24]). Given the retrospective, data-centric nature of our research, a consent waiver was granted.

For external validation, we used dataset of a prospective single center cohort, the Peking University First Hospital CKD cohort (PKUFH cohort) [18]. Peking University First Hospital established the first kidney division in China and is a kidney disease reference center with patients from all over China, particularly those from northern China. Between January 2013 and December 2021, a total of 1,115 adult patients with CKD stage 3-5 were registered in the cohort, being followed-up regularly every 3 to 6 months. Those with unclear patient state records ($n = 3$), incomplete follow-up data ($n=65$), or without ≥ 2 times of $eGFR \leq 60ml/min/1.73m^2$ separated by a period of ≥ 3 months to ≤ 2 years ($N=113$) are excluded, resulting in a total of 934 valid cases. Written informed consent was obtained from all participants for the use of clinical data in future studies upon they were registered in the cohort. The conduct of the study has been approved by the Ethics Committee of Peking University First Hospital (Approval ID: 2011[363]). The flow diagram of study participants selection is listed in Figure 1.

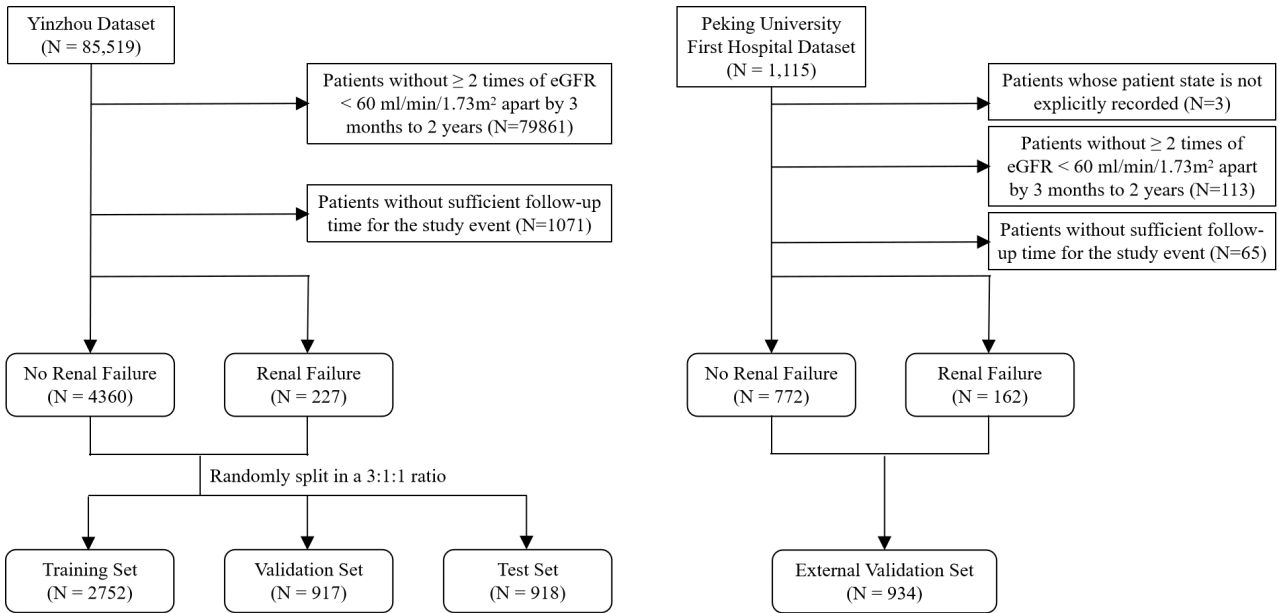


Figure 1: Flowchart of Study Enrollment and Inclusion Criteria.

2.2. Predictors and Outcomes

We select the eight variables in the KFREs for analysis [6], among which, six were set into time-series (eGFR, urine albumin-to-creatinine ratio [uACR], albumin, blood calcium, blood phosphorus, and HCO_3), while two were static variables (age and gender). For the CK-NET-Yinzhou cohort, the date of the second eligible eGFR was the index date, within half year prior to which, the baseline value of all other time-series variables were extracted with the closest records used. Thereafter, follow-up values were updated whenever there was

a value recorded. For the PKUFH cohort, all six time-series variables were recorded on the same date of baseline and each follow-up visit. eGFR is calculated using the serum creatinine-based CKD-EPI equation [19], as discussed in Appendix A. In the CK-NET-Yinzhou dataset, less than 10% of patients have uACR measured, so the missing measure is derived either from dipstick urinary protein or urine protein-to-creatinine ratio by using conversion equations [20], as discussed in Appendix B.

This study takes the initiation of maintenance dialysis (including hemodialysis and peritoneal dialysis) as the outcome. For the CK-NET-Yinzhou cohort, the outcome is identified according to the service items in medical billing with hemodialysis identified by claims records of hemodialyzer and related operations and peritoneal dialysis by that of peritoneal dialysis fluid. ICD codes are also used to ascertain dialysis-related diagnoses, as discussed in C.3. If diagnosis of acute kidney injury was detected (related ICD-10 codes are listed in D.4), the concurrent dialysis would not be labeled as outcome. Emigration to another city, death or reaching the specified length of follow-up (2 or 5 years) of KFREs were considered censoring [21]. For the PKUFH cohort, the ascertainment of the outcome was via scheduled follow-up in the clinic at a 3–6 month interval. The patients who cannot be got in touch with for ≥ 6 months were labeled as loss of follow-up. Medical records were requested to verify the initiation of maintenance dialysis. Loss of follow-up, death, reaching the specified length of follow-up or administered end of the current study (31st Dec. 2021), whichever came first, was treated as censoring.

2.3. Data Pre-processing

Data preprocessing for the proposed model includes deleting future data, determining the time scale for analysis, transforming the data structure and filling missing values. First, the date three months before that of dialysis was used as cut-off with the data afterwards deleted to avoid revealing future information. Second, we used month as the unit of time series variables’ time interval and merged the patient’s multiple measured data by calculating mean value within each unit, as shown in the process from (a) to (b) in Figure 2. The reason why we choose month as the time scale is discussed in Appendix E. Third, data was integrated into a multivariate irregular sampled missing matrix, as shown in (b) to (c). Fourth, missing data was filled with median of the variable values in the training set data. We select KFREs as the static baseline model. The index date is also used as the study index date, and variable values closest to this date within six months before or after are utilized.

2.4. Model Development

The CK-NET-Yinzhou dataset was randomly split into training, validation, and test sets in a 3:1:1 ratio, considering factors such as age, gender, occurrence of kidney failure, and mortality. Statistical comparison for the distribution of the variables (chi-square test for categorical variable and ANOVA for continuous variable) was conducted through the three datasets, revealing not any significant difference. Then, six time series variables from each patient, along with their time intervals, are fed into the Time-aware Long Short-Term Memory (T-LSTM) model [22] in a batch-wise manner.

T-LSTM is an extension of the traditional Long Short-Term Memory (LSTM) model [10] designed to handle irregular time intervals in time series data. In LSTM, the cell state C_t is updated using the following formula:

$$C_t = f_t \cdot C_{t-1} + i_t \cdot \tilde{C}_t, \quad (1)$$

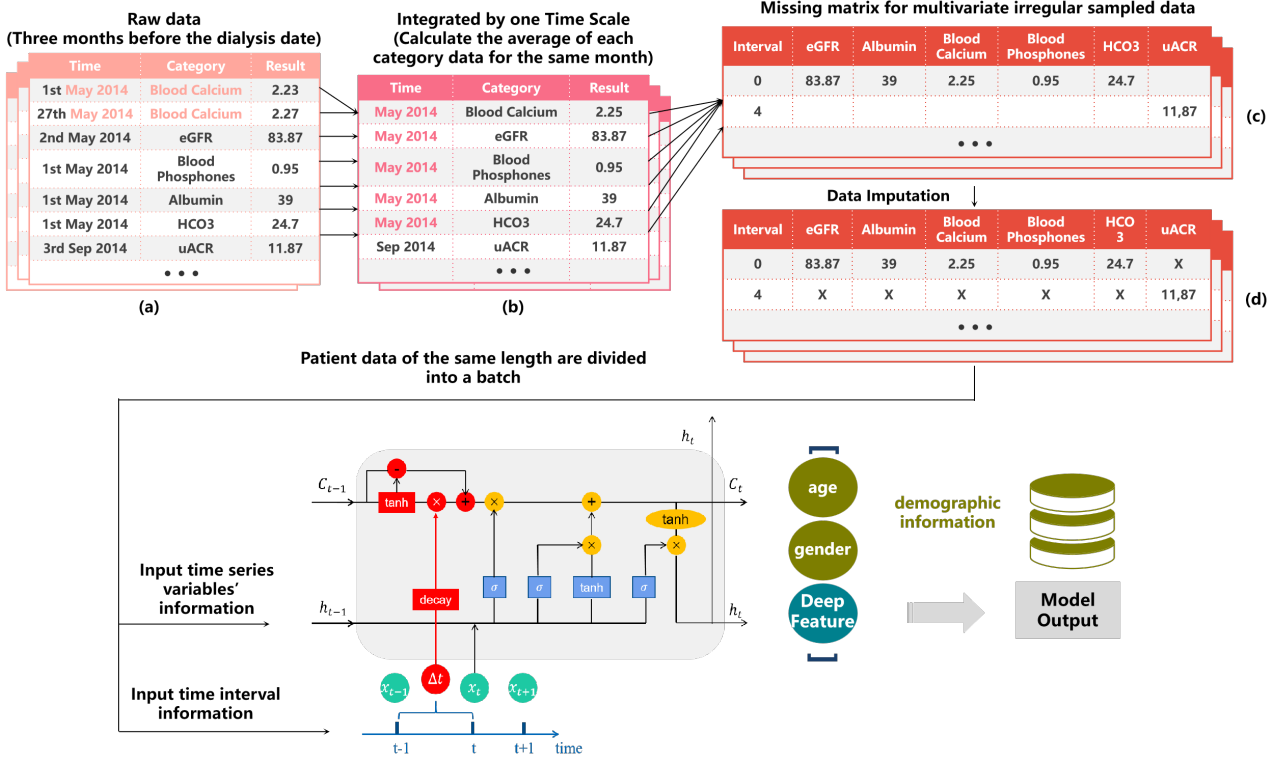


Figure 2: The Model Architecture.

Here, C_{t-1} is the previous cell state, f_t is the forget gate, which determines how much of the previous state is retained in the current state; i_t is the input gate, which controls the extent to which the current input affects the cell state; and \tilde{C}_t is the candidate cell state, computed based on the current input and the previous hidden state. Unlike standard LSTM, T-LSTM introduces a time decay mechanism to adjust the memory cell states based on the elapsed time between observations. The key modification introduces a time gate that modulates the LSTM cell states, and the updated cell state \tilde{C}_t is computed as follows:

$$\tilde{C}_t = C_t + f_t \cdot (g(\Delta t) - 1)C_{t-1}^S, \quad (2)$$

where $g(\Delta t)$ represents the time decay factor, Δt is the time gap between consecutive observations, and C_{t-1}^S is learnt from C_{t-1} . This mechanism allows T-LSTM to capture time-sensitive patterns in patient data more effectively. More details are explained in Appendix I.

The output from the T-LSTM model is a high-dimensional vector, which serves as the patient's deep feature. This deep feature is then concatenated with two static patient variables (age and gender). The concatenated vector is fed into a fully connected neural layer to get the final output: a value between 0 and 1, signifying the probability of a patient with CKD progressing into kidney failure.

2.5. Model Evaluation

To evaluate the model performance, we choose the Area Under the Receiver Operating Characteristic Curve (AUROC) with 95% confidence interval (CI) as the primary metric. The static and dynamic KFRE model [23] and the LSTM model [10] were chosen as baseline models. The static KFREs are linear models that calculated the risk of kidney failure; dynamic KFREs

update the patient’s risk by using the latest test results; the LSTM model is a basic time series model without considering the irregular intervals. We conducted a temporal comparative experiment across these models.

Simultaneously, a box plot was employed to illustrate the variance in the predictive values of models for patients who experienced kidney failure versus those who did not. The Decision Curve Analysis (DCA) curve can articulate optimal use cases by comparing the strategy using the prediction model to the “treat all” or “treat none” ones [24]. The x-axis of DCA represents the range of threshold probability and the y-axis provides the net benefit given specific threshold probability by taking into account both the true positive and false positive rates. We also created a calibration curve using 30 equally spaced quantiles to provide insights into the alignment between the model’s predicted probabilities and the observed frequencies.

2.6. Robustness Analysis

We undertook a subgroup analysis on the internal validation dataset, focusing on the demographic variables of age and gender. Gender is categorized as male or female, while age is segmented into the following groups: young (18-44 years old), middle-aged (45-59 years old), young-elderly (60-74 years old), and elderly (above 75 years old).

2.7. Model Interpretation

We employed the SHapley Additive exPlanations (SHAP) method [25] to calculate feature importance in the proposed model and to determine if the correlation between input features and the output is positive or negative. Moreover, we delved into the practical implication of the deep features. We employ the K-means algorithm to cluster the hidden layer vectors and applied the T-SNE method to reduce it to a 2-dimensional space and visualize the clustering results. In addition, we utilized radar and box plots to analyze the differences in variables and model predictions among the categories obtained from clustering.

2.8. Model Deployment

We explicitly extract the model weights and transform them into a set of visible equations (see in Appendix I). The model becomes fully interpretable and is not dependent on any specific deep learning architecture. Then, we deployed the KFDeep model on a web-based platform, enabling users to directly input a patient’s historical data for all eight indicators to calculate the risk of progression to kidney failure.

2.9. Role of the funding source

The funders of the study had no role in the study design, data collection, data analysis, data interpretation, or writing of the report.

3. Results

In the internal retrospective dataset, out of 85,519 individuals, 4,587 CKD patients were selected for modeling, including a training set (N=2,752), a validation set (N=917), and a testing set (N=918); In the external prospective dataset, out of 1,115 individuals, 934 patients were selected for validation. Table 1 presents the distribution of demographic metrics (continuous variables were represented by their median values and interquartile range(IQR)) and the P value across 3 internal sets.

Table 1: Baseline Characteristics of the Study Population.

	Training Set	Validation Set	Testing Set	External Set	P Value(Among internal sets)
Sample Size	2752	917	918	934	
Age	74 (68, 83)	74 (68, 83)	74 (68, 83)	67 (55, 80)	0.755
Female	1418 (52)	489 (53)	491 (53)	499 (53)	0.457
eGFR	59 (46, 74)	59 (47, 73)	60 (47, 73)	30 (16, 42)	0.584
uACR	11.9 (11.9, 25.2)	11.9 (11.9, 25.2)	11.9 (11.9, 25.2)	142.9 (25.2, 433.4)	0.828
Albumin	40.1 (36.2, 43.7)	40.1 (36.6, 43.8)	40.1 (36.6, 43.8)	42.6 (40.2, 44.7)	0.809
Blood Calcium	2.2 (2.1, 2.3)	2.2 (2.1, 2.3)	2.2 (2.1, 2.3)	2.3 (2.2, 2.4)	0.871
Blood Phosphorus	1.02 (0.91, 1.15)	1.02 (0.92, 1.16)	1.02 (0.92, 1.16)	1.19 (1.05, 1.35)	0.423
HCO3	24.7 (24.0, 24.7)	24.7 (24.0, 24.7)	24.7 (24.0, 24.7)	24.4 (22.2, 26.4)	0.158
Kidney Failure	137 (5)	45 (5)	45 (5)	162 (17)	0.993
Death	24 (0.87)	8 (0.87)	8 (0.87)	14 (1.5)	0.567
Length	11 (5, 14)	11 (5, 14)	11 (5, 14)	11 (5, 23)	0.356

Note: Continuous variables are presented as the median (25th and 75th interquartile range, IQR). Categorical variables are presented as counts (n) and percentages (%). "Length" refers to the length of the pre-processed patient data sequence. We utilize all electronic health record data from the patient's history, and therefore, we provide statistics on the average number of times each patient's data is used.

The experimental results for proposed model and baseline model are shown in Table 2. Our proposed model(KFDeep) showed the best performance in both internal and external validations.

Table 2: AUROC Scores of Baseline Models.

Model	Internal Validation	External Validation
KFRE (2 years 4 variables)	0.851 (0.815, 0.887)	0.700 (0.652, 0.748)
KFRE (2 years 8 variables)	0.862 (0.827, 0.897)	0.732 (0.685, 0.779)
KFRE (5 years 4 variables)	0.827 (0.789, 0.865)	0.690 (0.642, 0.738)
KFRE (5 years 8 variables)	0.836 (0.798, 0.874)	0.733 (0.686, 0.780)
LSTM (8 variables)	0.884 (0.851, 0.917)	0.776 (0.732, 0.820)
KFDeep (8 variables + time interval)	0.946 (0.922, 0.970)	0.805 (0.763, 0.847)

The results of dynamic comparative experiments were shown in the Figure3, and more results were detailed in Appendix H. In the internal dataset, when the x-axis was set to 6 months, KFRE used the same data range as the proposed model. In the external dataset, this alignment occurred when the x-axis was 1 month. It can be seen that our model performed better than static KFRE at this time. More importantly, our model demonstrated greater stability compared to the dynamic KFRE model. Additionally, as the range of data used expanded, the performance of our proposed model (KFDeep) improved further.

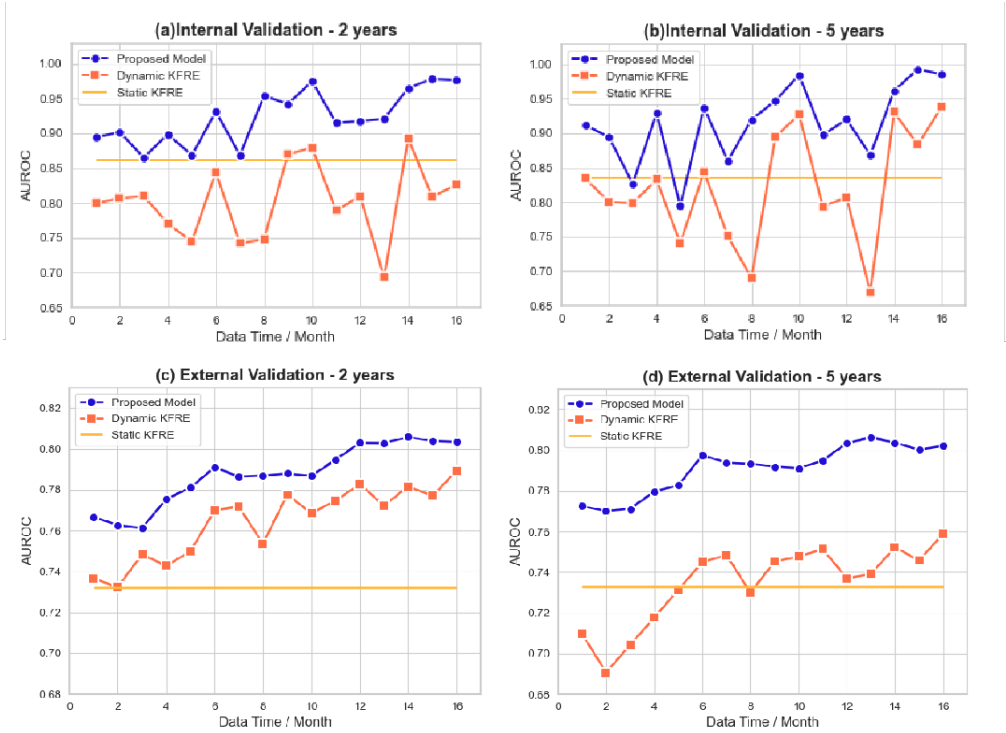


Figure 3: AUROC Comparison of Baseline Models Across Internal and External Validation over 2- and 5-Year Time Horizons.

We also evaluated the model’s performance across various scenarios. Figure 4(a) displays the distribution of the model’s output values for patients with kidney failure compared to those

without kidney failure in the CK-NET-Yinzhou test set. It’s evident that there’s a significant variance in the model’s output based on the presence or absence of kidney failure. This indicated that the magnitude of model output value can serve as an indicator of a patient’s risk for kidney failure. Figure 4(b) illustrates the DCA curve for the model’s internal validation dataset, showing that when the threshold is greater than 0.00625, making decisions using the KFDeep model can yield the better benefit than ”treat-all” and ”treat-none” strategy. Furthermore, Figure 4(c) depicts the calibration curve of the model’s internal validation dataset, demonstrating that the model’s predicted probabilities aligned well with actual observations.

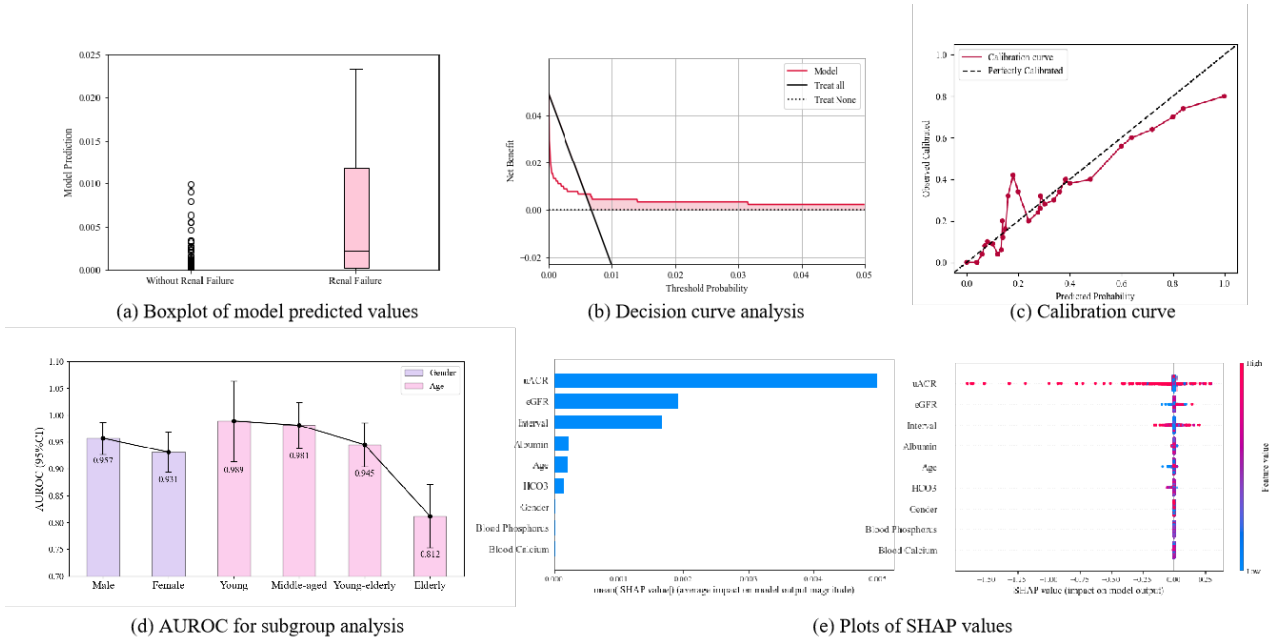


Figure 4: Analysis of Model Performance and Interpretability.

We verified the robustness of the model by subgroup analysis presented in Figure 4(d). In terms of gender, the overall performance remained balanced. Concerning age, the model’s predictive accuracy diminished as the patient’s age increased.

The interpretability of the model was also evaluated. Figure 4(e) showed the SHAP values of the model in the CK-NET-Yinzhou test set. According to the results of this experiment, we can find that uACR and eGFR were the two most important clinical indicators. Figure 5 (a) showed the clustering results of the deep features of the internal validation set. The deep features were divided into three clear categories. Figure 5 (b) showed the differences between the three types of patients in six time series variables by the clustering algorithm and the average value of the model output. Referring to Figure 5 (c), it can be seen that from cluster 1 to cluster 3, the average prediction value of the model and uACR continued to increase, while eGFR was constantly decreasing.

To demonstrate how the model works, we deployed the KFDeep model on a web-based platform that does not rely on any deep learning frameworks. A more detailed demonstration of the web calculator is presented in Appendix K.

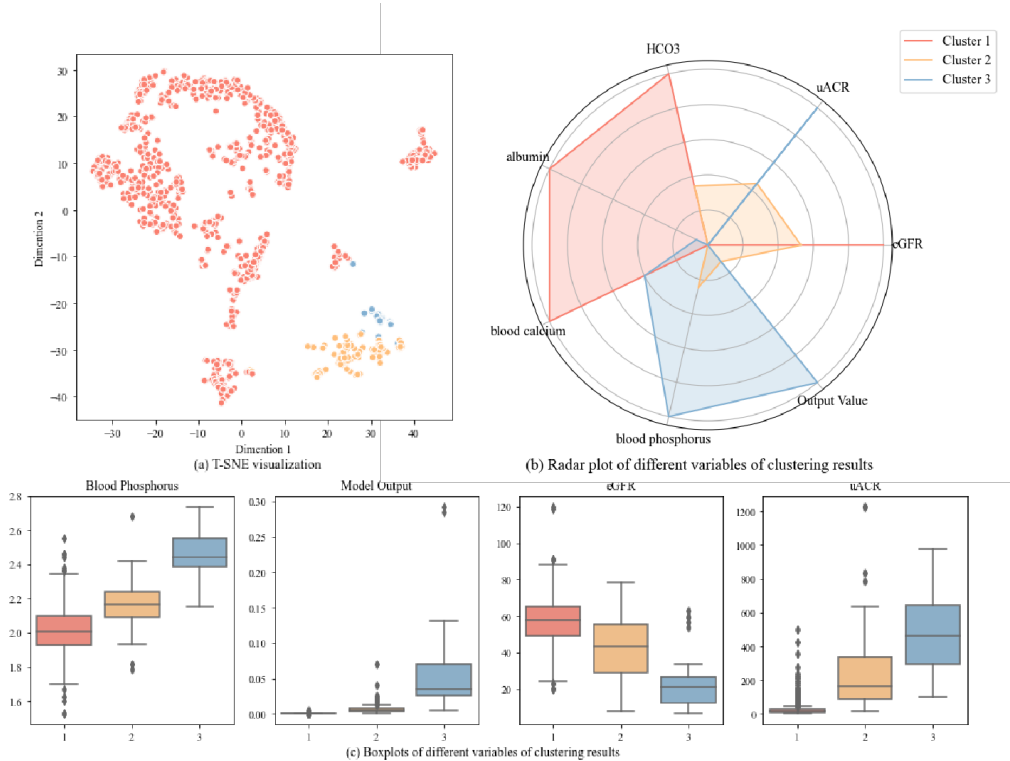


Figure 5: Deep Features Analysis.

4. Discussion

We developed a dynamic risk prediction framework, the KFDeep model, for kidney failure in a 2-year or 5-year time horizons for patients with CKD stage 3-5. The model was developed based on an EHR-based CKD registry in a coastal city of China and externally validated in a hospital-based CKD cohort. The model was featured with its simplicity, involving the eight variables in KFREs, and high accuracy, performing better than original static and dynamic KFREs. As the model can be expressed through several formulas, we deployed it as an easy-to-use and interpretable web-based tool, potentially facilitating optimal management of patients with CKD.

By continuously tracking common clinical indicators over time [26, 27], the developed KFDeep model can provide dynamic, real-time updates on the likelihood of kidney failure. Additionally, KFDeep was notable for being able to consider the temporal intervals between patient health assessments by using T-LSTM model. Comparing to the standard LSTM model [10], which does not include time intervals, it was revealed that KFDeep outperformed the model by 6.2% in internal datasets and 2.9% in external datasets in terms of AUROC. These findings underscored that the time intervals between health assessments in patients with CKD were crucial in reflecting the progression of CKD. Furthermore, unlike traditional dynamic models, which often suffered from computational complexity and can be difficult to implement in clinical practice [23, 28], KFDeep was designed to be computationally efficient with its structure clearly expressed in mathematical terms. This feature simplified its use and enhanced its practical applicability in clinical settings, thus probably offering physicians timely information for clinical decision-making.

Moreover, KFDeep has achieved state-of-the-art accuracy in predicting the progression of

CKD to kidney failure. Prior to the development of KFDeep, predictions of CKD progression primarily relied on static KFREs due to their internationally verified discriminative ability[7]. Compared to the KFREs, KFDeep demonstrated an average improvement of 10% in AUROC in internal validation dataset and 8% in external validation dataset. We did not compare KFDeep with other machine learning methods as their accuracy was equal to or inferior to that of KFREs [29, 30]. However, given KFDeep’s dynamic nature, we compared it with the dynamic KFRE model. KFDeep model exhibited superior performance, with an average increase of accuracy of 12.1% and 9.3% for predicting kidney failure within 2-year or 5-year, respectively, in the internal validation dataset, and 2.0% and 5.4%, respectively, in the external dataset. Additionally, KFDeep demonstrated greater stability in terms of accuracy with the use of longitudinal dynamic data. For instance, in the external validation dataset, KFDeep showed a 3.5% increase in prediction accuracy using 12 months of data and a 4.6% increase using 15 months of data than just using one month of data. This increased accuracy may be due to the dynamic model can update prediction results by using time series data and thus provide risk estimation more closer to the actual risk of the outcome.

A significant barrier to the use of deep learning models in medical applications is lack of interpretability [31]. However, KFDeep exhibited robust interpretability features. SHAP analysis has identified eGFR and uACR as critical factors in predicting kidney failure. Moreover, our deep feature clustering experiments categorized data into three groups, which also demonstrated that the risk of kidney failure within these clusters increased progressively with the eGFR declining and uACR increasing. These findings aligned with the findings of previous studies[32, 33]. In terms of the complication of CKD, we observed the average levels of blood phosphorus increased with the three clusters[34].

To facilitate the use of KFDeep, we deployed the model in a publicly accessible website, which also demonstrated the model was readily available for integration into healthcare systems as a user-friendly tool. With each update of test results, KFDeep would automatically recalculate the patient’s risk of progressing to kidney failure. This function can ensure healthcare providers are able to access to the most recent data-driven insights and enable them make timely informed clinical decisions. Future clinical trials are warranted to assess whether use of KFDeep, especially embedded into the health information system, can improve the guideline concordant clinical practice and, ultimately, clinical outcomes of patients with CKD.

This study has several limitations. First, the accuracy of our model decreased with increasing age. This may be because elderly patients have more significant competing risk of death than reaching kidney failure, such as mortality from cardiovascular diseases. In the future, we plan to develop more targeted models to improve predicting accuracy in the elderly population. Second, the study population predominantly comprised Chinese individuals, resulting in a homogeneous ethnic group and possibly constraining the model’s generalisability to other ethnic groups. External validations in diverse populations were warranted. Third, though the clustering results of the estimated risk showed high consistency with eGFR and uACR, the key marker for severity of CKD, our analysis was primarily based on correlational data and the interpreted relationship may not be interpreted as causality. We plan to explore these causal relationships in future prospective studies.

5. Conclusion

In this study, we developed and validated an easy to-use model to provide dynamic individual predictions of risk of kidney failure for patients with CKD. We showed its validity

in external validation and multiple evaluation experiments. We also deployed it on a web-based platform to showcase its practical utility. This model can be seamlessly integrated into healthcare systems to assist physicians in making accurate and timely decisions regarding management of patients.

6. Acknowledgement

Shenda Hong is supported by the National Natural Science Foundation of China (62102008). Jinwei Wang is supported by National High Level Hospital Clinical Research Funding (Interdepartmental Research Project of Peking University First Hospital: 2024IR14), CAMS Innovation Fund for Medical Sciences (2019-I2M-5-046) and State Key Laboratory of Vascular Homeostasis and Remodeling, Peking University. Luxia Zhang is supported by the National Natural Science Foundation of China (72125009), CAMS Innovation Fund for Medical Sciences (2019-I2M-5-046) and State Key Laboratory of Vascular Homeostasis and Remodeling, Peking University.

References

- [1] K. J. Foreman, N. Marquez, A. Dolgert, K. Fukutaki, N. Fullman, M. McGaughey, M. A. Pletcher, A. E. Smith, K. Tang, C.-W. Yuan, et al., Forecasting life expectancy, years of life lost, and all-cause and cause-specific mortality for 250 causes of death: reference and alternative scenarios for 2016–40 for 195 countries and territories, *The Lancet* 392 (10159) (2018) 2052–2090.
- [2] B. Bikbov, C. A. Purcell, A. S. Levey, M. Smith, A. Abdoli, M. Abebe, O. M. Adebayo, M. Afarideh, S. K. Agarwal, M. Agudelo-Botero, et al., Global, regional, and national burden of chronic kidney disease, 1990–2017: a systematic analysis for the global burden of disease study 2017, *The lancet* 395 (10225) (2020) 709–733.
- [3] C. K. D. P. Consortium, et al., Association of estimated glomerular filtration rate and albuminuria with all-cause and cardiovascular mortality in general population cohorts: a collaborative meta-analysis, *The Lancet* 375 (9731) (2010) 2073–2081.
- [4] S. Van Laecke, E. V. Nagler, F. Verbeke, W. Van Biesen, R. Vanholder, Hypomagnesemia and the risk of death and gfr decline in chronic kidney disease, *The American journal of medicine* 126 (9) (2013) 825–831.
- [5] D. C. Crews, A. K. Bello, G. Saadi, Burden, access, and disparities in kidney disease, *Brazilian Journal of Medical and Biological Research* 52 (2019).
- [6] N. Tangri, L. A. Stevens, J. Griffith, H. Tighiouart, O. Djurdjev, D. Naimark, A. Levin, A. S. Levey, A predictive model for progression of chronic kidney disease to kidney failure, *Jama* 305 (15) (2011) 1553–1559.
- [7] N. Tangri, M. E. Grams, A. S. Levey, J. Coresh, L. J. Appel, B. C. Astor, G. Chodick, A. J. Collins, O. Djurdjev, C. R. Elley, et al., Multinational assessment of accuracy of equations for predicting risk of kidney failure: a meta-analysis, *Jama* 315 (2) (2016) 164–174.

- [8] D. Dai, P. J. Alvarez, S. D. Woods, A predictive model for progression of chronic kidney disease to kidney failure using a large administrative claims database, *ClinicoEconomics and Outcomes Research* (2021) 475–486.
- [9] D. K. Lim, J. H. Boyd, E. Thomas, A. Chakera, S. Tippaya, A. Irish, J. Manuel, K. Betts, S. Robinson, Prediction models used in the progression of chronic kidney disease: A scoping review, *PLoS One* 17 (7) (2022) e0271619.
- [10] S. Hochreiter, Long short-term memory, *Neural Computation* MIT-Press (1997).
- [11] A. Azhie, D. Sharma, P. Sheth, F. A. Qazi-Arisar, R. Zaya, M. Naghibzadeh, K. Duan, S. Fischer, K. Patel, C. Tsien, et al., A deep learning framework for personalised dynamic diagnosis of graft fibrosis after liver transplantation: a retrospective, single canadian centre, longitudinal study, *The Lancet Digital Health* 5 (7) (2023) e458–e466.
- [12] S. E. Khorsandi, Will deep learning change outcomes in liver transplant?, *The Lancet Digital Health* 5 (7) (2023) e398–e399.
- [13] J. Wang, B. Bao, P. Shen, G. Kong, Y. Yang, X. Sun, G. Ding, B. Gao, C. Yang, M. Zhao, et al., Using electronic health record data to establish a chronic kidney disease surveillance system in china: protocol for the china kidney disease network (ck-net)-yinzhou study, *BMJ open* 9 (8) (2019) e030102.
- [14] G. S. Collins, J. B. Reitsma, D. G. Altman, K. G. Moons, Transparent reporting of a multivariable prediction model for individual prognosis or diagnosis (tripod) the tripod statement, *Circulation* 131 (2) (2015) 211–219.
- [15] H. Lin, X. Tang, P. Shen, D. Zhang, J. Wu, J. Zhang, P. Lu, Y. Si, P. Gao, Using big data to improve cardiovascular care and outcomes in china: a protocol for the chinese electronic health records research in yinzhou (cherry) study, *BMJ open* 8 (2) (2018) e019698.
- [16] H.-Y. Wang, J. Du, Y. Yang, H. Lin, B. Bao, G. Ding, C. Yang, G. Kong, L. Zhang, Rapid identification of chronic kidney disease in electronic health record database using computable phenotype combining a common data model, *Chinese Medical Journal* 136 (7) (2023) 874–876.
- [17] H.-Y. Wang, G.-H. Ding, H. Lin, X. Sun, C. Yang, S. Peng, J. Wang, J. Du, Y. Zhao, Z. Chen, et al., Influence of doctors’ perception on the diagnostic status of chronic kidney disease: results from 976 409 individuals with electronic health records in china, *Clinical Kidney Journal* 14 (11) (2021) 2428–2436.
- [18] X. Deng, B. Gao, F. Wang, M.-h. Zhao, J. Wang, L. Zhang, Red blood cell distribution width is associated with adverse kidney outcomes in patients with chronic kidney disease, *Frontiers in Medicine* 9 (2022) 877220.
- [19] A. S. Levey, L. A. Stevens, C. H. Schmid, Y. Zhang, A. F. Castro III, H. I. Feldman, J. W. Kusek, P. Eggers, F. Van Lente, T. Greene, et al., A new equation to estimate glomerular filtration rate, *Annals of internal medicine* 150 (9) (2009) 604–612.

- [20] K. Sumida, G. N. Nadkarni, M. E. Grams, Y. Sang, S. H. Ballew, J. Coresh, K. Matsushita, A. Surapaneni, N. Brunskill, S. J. Chadban, et al., Conversion of urine protein–creatinine ratio or urine dipstick protein to urine albumin–creatinine ratio for use in chronic kidney disease screening and prognosis: an individual participant–based meta-analysis, *Annals of internal medicine* 173 (6) (2020) 426–435.
- [21] L. Pan, J. Wang, Y. Deng, Y. Sun, Z. Nie, X. Sun, C. Yang, G. Ding, M.-H. Zhao, Y. Liao, et al., External validation of the kidney failure risk equation among urban community-based chinese patients with ckd, *Kidney Medicine* 6 (5) (2024) 100817.
- [22] I. M. Baytas, C. Xiao, X. Zhang, F. Wang, A. K. Jain, J. Zhou, Patient subtyping via time-aware lstm networks, in: *Proceedings of the 23rd ACM SIGKDD international conference on knowledge discovery and data mining*, 2017, pp. 65–74.
- [23] N. Tangri, L. A. Inker, B. Hiebert, J. Wong, D. Naimark, D. Kent, A. S. Levey, A dynamic predictive model for progression of ckd, *American Journal of Kidney Diseases* 69 (4) (2017) 514–520.
- [24] A. J. Vickers, B. van Calster, E. W. Steyerberg, A simple, step-by-step guide to interpreting decision curve analysis, *Diagnostic and prognostic research* 3 (2019) 1–8.
- [25] S. M. Lundberg, S.-I. Lee, A unified approach to interpreting model predictions, *Advances in neural information processing systems* 30 (2017).
- [26] M. Raynaud, O. Aubert, G. Divard, P. P. Reese, N. Kamar, D. Yoo, C.-S. Chin, É. Bailly, M. Buchler, M. Ladrière, et al., Dynamic prediction of renal survival among deeply phenotyped kidney transplant recipients using artificial intelligence: an observational, international, multicohort study, *The Lancet Digital Health* 3 (12) (2021) e795–e805.
- [27] P. Schwab, A. Mehrjou, S. Parbhoo, L. A. Celi, J. Hetzel, M. Hofer, B. Schölkopf, S. Bauer, Real-time prediction of covid-19 related mortality using electronic health records, *Nature communications* 12 (1) (2021) 1058.
- [28] D. Xie, W. Yang, C. Jepson, J. Roy, J. Y. Hsu, H. Shou, A. H. Anderson, J. R. Landis, H. I. Feldman, Statistical methods for modeling time-updated exposures in cohort studies of chronic kidney disease, *Clinical journal of the American Society of Nephrology: CJASN* 12 (11) (2017) 1892.
- [29] M. Wainstein, A. K. Rahimi, I. Katz, H. Healy, S. Pirabhahar, K. Turner, S. Shrapnel, A comparison between a random forest model and the kidney failure risk equation to predict progression to kidney failure, *medRxiv* (2023) 2023–05.
- [30] Q. Bai, C. Su, W. Tang, Y. Li, Machine learning to predict end stage kidney disease in chronic kidney disease, *Scientific reports* 12 (1) (2022) 8377.
- [31] S. Tonekaboni, S. Joshi, M. D. McCradden, A. Goldenberg, What clinicians want: contextualizing explainable machine learning for clinical end use, in: *Machine learning for healthcare conference*, PMLR, 2019, pp. 359–380.
- [32] P. Cockwell, L.-A. Fisher, The global burden of chronic kidney disease, *The Lancet* 395 (10225) (2020) 662–664.

- [33] J. J. Carrero, M. E. Grams, Y. Sang, J. Ärnlöv, A. Gasparini, K. Matsushita, A. R. Qureshi, M. Evans, P. Barany, B. Lindholm, et al., Albuminuria changes are associated with subsequent risk of end-stage renal disease and mortality, *Kidney international* 91 (1) (2017) 244–251.
- [34] F. C. Barreto, D. V. Barreto, Z. A. Massy, T. B. Drüeke, Strategies for phosphate control in patients with ckd, *Kidney international reports* 4 (8) (2019) 1043–1056.

Appendix A. CKD-EPI Equation

For females:

$$eGFR = \begin{cases} 144 \times \left(\frac{\text{serum creatinine}}{88.4 \times 0.7}\right)^{-0.329} \times 0.993^{\text{age}}, & \text{if } \frac{\text{serum creatinine}}{88.4} \leq 0.7, \\ 144 \times \left(\frac{\text{serum creatinine}}{88.4 \times 0.7}\right)^{-1.209} \times 0.993^{\text{age}}, & \text{otherwise.} \end{cases} \quad (\text{A.1})$$

For males:

$$eGFR = \begin{cases} 141 \times \left(\frac{\text{serum creatinine}}{88.4 \times 0.9}\right)^{-0.411} \times 0.993^{\text{age}}, & \text{if } \frac{\text{serum creatinine}}{88.4} \leq 0.9, \\ 141 \times \left(\frac{\text{serum creatinine}}{88.4 \times 0.9}\right)^{-1.209} \times 0.993^{\text{age}}, & \text{otherwise.} \end{cases} \quad (\text{A.2})$$

Appendix B. Equation for uACR Conversion

The equation of calculating uACR based on dipstick urinary protein is:

$$uACR = \exp \left(\begin{aligned} &2.4738 \\ &+ 0.7539 \times (\text{if trace}) \\ &+ 1.7243 \times (\text{if } +) \\ &+ 3.3475 \times (\text{if } ++) \\ &+ 4.6399 \times (\text{if } >++) \end{aligned} \right). \quad (\text{B.1})$$

The equation of calculating uACR based on urine protein-to-creatinine ratio (PCR) is:

$$uACR = \exp \left(\begin{aligned} &5.3920 \\ &+ 0.3072 \cdot \log\left(\min\left(\frac{PCR}{50}, 1\right)\right) \\ &+ 1.5793 \cdot \log\left(\max\left(\min\left(\frac{PCR}{500}, 1\right), 0.1\right)\right) \\ &+ 1.1266 \cdot \log\left(\max\left(\frac{PCR}{500}, 1\right)\right) \end{aligned} \right). \quad (\text{B.2})$$

Appendix C. The ICD-10 codes used for identifying dialysis patients

The ICD-10 codes used for identifying dialysis patients are shown in Table C.3

Table C.3: ICD-10 codes for dialysis modality

Dialysis modality	ICD-10 codes		
	National version		Beijing version
HD	T80.801, T80.902, T82.400, T82.401, Z99.201		T82.401, Z99.201
PD	T85.609, T85.610, T85.611, T85.710, T85.711, T85.801, T85.901, Z49.201		T80.201, T85.602, Z49.201, Z99.202

Abbreviations: HD, hemodialysis; PD, peritoneal dialysis; ICD-10, International Classification of Diseases-10.

Appendix D. The ICD-10 Codes used for Identifying Patients with Cute Kidney Injury

The ICD-10 codes used for identifying patients with acute kidney injury are shown in Table D.4.

Table D.4: ICD-10 Codes for Acute Kidney Injury

ICD-10 codes	
National version	Beijing version
N17, N01, T79.5, D59.3, K76.7, O90.4, N96.x00, A23.100, O00.101, O00.105, O00.108, O00.111, O00.114, O02.001, O02.100, O03, O04, O05, O06.900, O07, O08 (exclude O08.006, O08.103, O08.104, O08.105, O08.106, O08.302, O08.806), O20.000, O26.200, O31.100, Z09.802, Z35.100, Z35.101, Z35.104, N10.x00, N10.x01, N99.000, N99.001	N17, N01, T79.5, D59.3, K76.7, O90.4, N96xx01, O00.102, O00.107, O00.110, O00.111, O02.101, O03, O04 (exclude O04.905, O04.907), O05, O06 (exclude O06.907, O06.908) O07, O08 (exclude O08.103, O08.105, O08.301, O08.801, O08.803, O08.806, O08.807, O08.809) O20.001, O26.201, Z30.201, Z35.102, Z98.8308, Z98.8312, N00.908, N10xx03, N10xx04+H20.9

Abbreviations: ICD-10, International Classification of Diseases-10.

Appendix E. Time Scale Chosen

The appropriate time scale has a great impact on modeling. That's because if the time scale is too short, more variables will be missing under the same timestamp, that is, there will be more peacock values in Figure 2 (c); if the time scale is too long, more data will need to be merged, resulting in information loss. As a result, we compare three time scales: day, month, and year to balance the missing rate and merging rate of variables, and select month as the time scale.

The missing rates of variables at different time scales are shown in Table E.5. It can be seen that choosing day as the time scale results in an excessively high missing rate. However, choosing year as the time scale would significantly shorten the length of the time series, as the Figure E.6 shown. Considering both the missing rate and the length of the time series, selecting month as the time scale is the most appropriate.

Table E.5: The Missing Rates of Variables at Different Time Scales.

Time scale	eGFR	uACR	Albumin	Blood calcium	Blood phosphorus	HCO ₃
Day	41.4%	57.8%	51.0%	43.6%	51.2%	40.6%
Month	27.8%	41.3%	35.8%	37.1%	43.7%	35.2%
Year	20.0%	32.2%	23.8%	29.6%	35.8%	33.8%

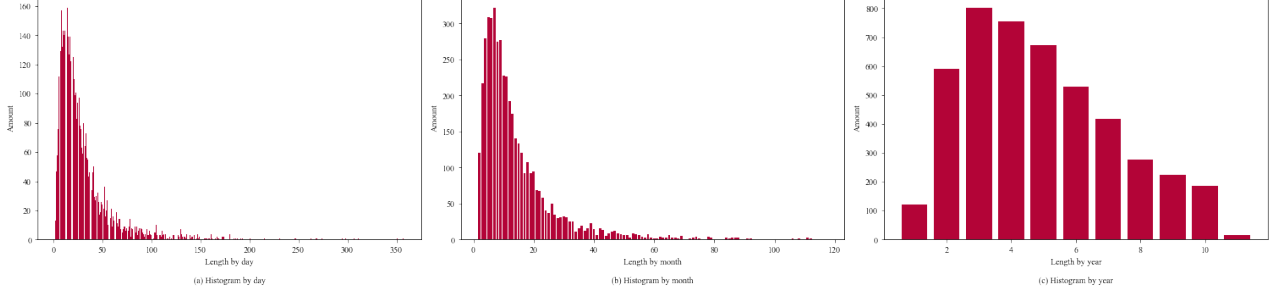


Figure E.6: Histogram of data length by different time scales

Appendix F. Forms of Non-North America calibrated Kidney Failure Risk Equations (KFREs)

$$\begin{aligned}
 \text{KFRE 4-variable 2-year probability} &= 1 - 0.9832^{\exp(-0.2201 \times (\text{age}/10 - 7.036))} \\
 &+ 0.2467 \times (\text{male} - 0.5642) \\
 &- 0.5567 \times \exp(\text{eGFR}/5 - 7.222) \\
 &+ 0.4510 \times (\log(\text{ACR}) - 5.137),
 \end{aligned} \tag{F.1}$$

$$\begin{aligned}
 \text{KFRE 8-variable 2-year probability} &= 1 - 0.9827^{\exp(-0.1992 \times (\text{age}/10 - 7.036))} \\
 &+ 0.1602 \times (\text{male} - 0.5642) \\
 &- 0.4919 \times \exp(\text{eGFR}/5 - 7.222) \\
 &+ 0.3364 \times (\log(\text{ACR}) - 5.137) \\
 &- 0.3441 \times (\text{albumin} - 3.997) \\
 &+ 0.2604 \times (\text{phosphate} - 3.916) \\
 &- 0.07354 \times (\text{HCO}_3 - 25.57) \\
 &- 0.2228 \times (\text{calcium} - 9.355),
 \end{aligned} \tag{F.2}$$

$$\begin{aligned}
 \text{KFRE 4-variable 5-year probability} &= 1 - 0.9365^{\exp(-0.2201 \times (\text{age}/10 - 7.036))} \\
 &+ 0.2467 \times (\text{male} - 0.5642) \\
 &- 0.5567 \times \exp(\text{eGFR}/5 - 7.222) \\
 &+ 0.4510 \times (\log(\text{ACR}) - 5.137),
 \end{aligned} \tag{F.3}$$

Table G.6: P Values of Variables and Model Output.

Variable	P value
Blood Calcium	0.014
HCO3	0.028
Age	0.034
Albumin	0.046
Gender	0.055
Blood Phosphorus	0.069
eGFR	0.082
uACR	0.093

$$\begin{aligned}
 \text{KFRE 8-variable 5-year probability} = & 1 - 0.9245^{\exp(-0.1992 \times (\text{age}/10 - 7.036))} \\
 & + 0.1602 \times (\text{male} - 0.5642) \\
 & - 0.4919 \times \exp(\text{eGFR}/5 - 7.222) \\
 & + 0.3364 \times (\log(\text{ACR}) - 5.137) \\
 & - 0.3441 \times (\text{albumin} - 3.997) \\
 & + 0.2604 \times (\text{phosphate} - 3.916) \\
 & - 0.07354 \times (\text{HCO3} - 25.57) \\
 & - 0.2228 \times (\text{calcium} - 9.355).
 \end{aligned} \tag{F.4}$$

Appendix G. Statistical Relationship Between Predictors and Model Prediction

We use the model prediction value as the outcome and test the statistical relationship between this value and eight variables. For the 6 time series variables, the average value of multiple data is taken for testing. Table G.6 shows the P values between the model output value and the eight predictors selected in this study. All P values are less than 0.1, and the P values of four indicators are less than 0.05. This indicates that the model output contains information about the predictors.

Appendix H. Dynamic Comparative Experiments

Table H.7 and H.8 presents the detailed AUROC scores of dynamic comparative experiments in internal and external validation data respectively.

Appendix I. Model Details

The KFDeep model can calculate the risk ratio of patients with CKD for kidney failure based on patients' electronic health records. The patient's EHR data is represented as follows:

$$\text{EHR} = [\text{EHR}_{t_0}, \dots, \text{EHR}_{t_n}]^\top, \tag{I.1}$$

where the EHR_{t_n} can be represented as:

$$\text{EHR}_{t_i} = [\Delta t_{t_i}, \text{eGFR}_{t_i}, \text{Albumin}_{t_i}, \text{Blood Calcium}_{t_i}, \text{Blood Phosphorus}_{t_i}, \text{uACR}_{t_i}, \text{HCO3}_{t_i}]^\top, \tag{I.2}$$

Table H.7: AUROC Scores of Internal Validation Dataset.

Month	Internal data	Internal data	Internal data	Internal data
	- 2 year (proposed model)	- 2 year (dynamic KFRE model)	- 5 year (proposed model)	- 5 year (dynamic KFRE model)
1	0.894	0.799	0.672	0.912
2	0.902	0.807	0.672	0.894
3	0.865	0.810	0.670	0.827
4	0.899	0.771	0.671	0.930
5	0.868	0.744	0.679	0.795
6	0.931	0.844	0.682	0.937
7	0.868	0.742	0.697	0.860
8	0.954	0.748	0.693	0.920
9	0.942	0.870	0.693	0.947
10	0.975	0.880	0.691	0.985
11	0.915	0.789	0.691	0.897
12	0.917	0.810	0.694	0.920
13	0.921	0.693	0.703	0.868
14	0.965	0.893	0.706	0.962
15	0.978	0.809	0.703	0.993
16	0.977	0.826	0.700	0.985

where Δt represents the time interval between patients' assessment. When $i = 0$, the $\Delta t_{t_0} = 0$; when $i > 0$, the Δt_{t_i} is the difference in months between the occurrence time of EHR_{t_i} and the occurrence time of $\text{EHR}_{t_{i-1}}$.

Send each of EHR_{t_0} to EHR_{t_n} sequentially into the following formula for iterative calculation. At each moment t , the calculation formula can be represented as:

$$C_{t-1}^S = \tanh(W_d C_{t-1} + b_d), \quad (\text{I.3})$$

$$g(\Delta t_{t_i}) = \frac{1}{\Delta t_{t_i} + 0.00001}, \quad (\text{I.4})$$

$$\hat{C}_{t-1}^S = C_{t-1}^S * g(\Delta t_{t_i}), \quad (\text{I.5})$$

$$C_{t-1}^T = C_{t-1} - C_{t-1}^S, \quad (\text{I.6})$$

$$C_{t-1}^* = C_{t-1}^T + \hat{C}_{t-1}^S, \quad (\text{I.7})$$

$$f_t = \sigma(\mathbf{W}_f \text{EHR}_t + \mathbf{U}_f h_{t-1} + \mathbf{b}_f), \quad (\text{I.8})$$

$$i_t = \sigma(\mathbf{W}_i \text{EHR}_t + \mathbf{U}_i h_{t-1} + \mathbf{b}_i), \quad (\text{I.9})$$

$$o_t = \sigma(\mathbf{W}_o \text{EHR}_t + \mathbf{U}_o h_{t-1} + \mathbf{b}_o), \quad (\text{I.10})$$

Table H.8: AUROC Scores of External Validation Dataset.

Month	External data	External data	External data	External data
	- 2 year (proposed model)	- 2 year (dynamic KFRE model)	- 5 year (proposed model)	- 5 year (dynamic KFRE model)
1	0.759	0.736	0.772	0.709
2	0.766	0.732	0.772	0.690
3	0.762	0.748	0.770	0.704
4	0.761	0.742	0.771	0.717
5	0.775	0.749	0.779	0.731
6	0.780	0.769	0.782	0.745
7	0.790	0.771	0.797	0.748
8	0.786	0.753	0.793	0.730
9	0.786	0.777	0.793	0.745
10	0.787	0.768	0.791	0.747
11	0.786	0.774	0.791	0.751
12	0.794	0.782	0.794	0.737
13	0.802	0.772	0.803	0.739
14	0.802	0.781	0.806	0.752
15	0.805	0.776	0.803	0.745
16	0.803	0.789	0.800	0.759

$$\tilde{C} = \tanh(\mathbf{W}_c \text{EHR}_t + \mathbf{U}_c h_{t-1} + \mathbf{b}_c), \quad (\text{I.11})$$

$$C_t = f_t * C_{t-1}^* + i_t * \tilde{C}, \quad (\text{I.12})$$

$$h_t = o_t * \tanh(C_t). \quad (\text{I.13})$$

The $W_d, b_d, W_f, U_f, b_f, W_i, U_i, b_i, W_o, U_o, b_o, W_c, U_c, b_c$ are all constant matrices trained by the neural network. When $t = 0$, both C_0 and h_0 are initialized as zero matrices. The \tanh and σ functions used in the above formula are as follows:

$$\tanh(x) = \frac{e^x - e^{-x}}{e^x + e^{-x}}, \quad (\text{I.14})$$

$$\sigma(x) = \frac{1}{1 + e^{-x}}. \quad (\text{I.15})$$

The obtained C_t, h_t , and EHR_{t+1} are then used together as inputs for the next time step, until h_n is calculated.

$$h_b = f(\mathbf{W}_1 h_n + \mathbf{b}_1), \quad (\text{I.16})$$

where h_b is the final embedding. Then, concatenate the patient's static variables (gender and age) to h_b to obtain the h_a variable:

$$h_a = [h_b^\top, \text{age}, \text{gender}]^\top. \quad (\text{I.17})$$

Then, h_a is input into the following formula to obtain the final prediction:

$$\text{prediction} = \sigma(f(\mathbf{W}_2 h_a + \mathbf{b}_2)). \quad (\text{I.18})$$

Similarly, W_1, b_1, W_2, b_2 are also constant matrices obtained by neural network training. The final prediction is a 2-dimensional output, and we can obtain the probability distribution by the following equation:

$$p_1 = \text{softmax}(\text{prediction}_1), \quad (\text{I.19})$$

where the softmax function is as follows:

$$\text{Softmax}(\text{prediction}_i) = \frac{e^{\text{prediction}_i}}{\sum_{j=1}^n e^{\text{prediction}_j}}, \quad (\text{I.20})$$

where prediction_i represents the i -th element of the prediction variable.

Finally, we calibrated the model's output by quantiles to obtain risk values between 0 and 1. For example, if the risk is 0.6, it indicates that the individual has a higher risk of kidney failure than 60% of the population.

Appendix J. Case Study

We perform a detailed case study to ascertain whether the model's predictions truly reflect the real-time risk of a patient advancing to kidney failure, randomly selecting a patient whose data record exceeded the average entries. By tracking the model's output over successive time intervals, we observed the interplay between these probabilities and changes in the eGFR variable, whose diminishment is indicative of a more advanced stage of CKD. One patient's data, including outputs from the model and eGFR values, is presented in Figure J.7. We observe that as the eGFR declines and the patient's CKD severity escalates, the model's predicted risk of kidney failure concomitantly increases.

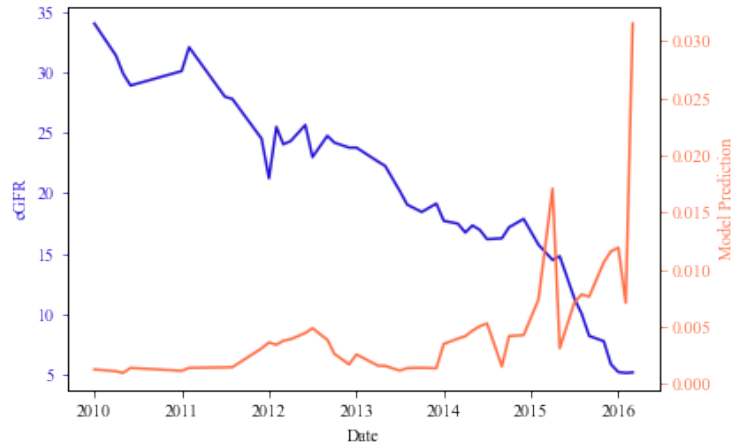


Figure J.7: Case Study: A Patient's Model Output and eGFR Curve.

Appendix K. Deployment

We deploy the KFDeep model on the website <https://visdata.bjmu.edu.cn/kfdeep>, where users can input a patient's complete historical EHR data to calculate the risk of progression to kidney failure. There are two usage options: one involves entering the data directly on the

website, and the other involves uploading the data in a table format. Figure K.8 illustrates how to input data directly, while Figure K.9 demonstrates the use of table-based input. Additionally, we provide a demo dataset, and upon inputting it, users can obtain results as shown in Figure K.10.

KFDeep: a Deep Dynamic Kidney Failure Prediction Model

Instruction

```

graph TD
    A[Choose DataUpload Method] --> B[Manual Entry]
    A --> C[Upload Form]
    B --> D[Fill as Required]
    C --> E[Download Template]
    E --> F[Fill as Required]
    F --> G[Upload Data]
    D --> H[Risk Assessment]
    G --> H
    
```

Data Upload

[Manual Entry](#) | [Upload Form](#)

* Age:

* Gender: male female

* Date	eGFR (mL/min/1.73 m ²)	Albumin (g/L)	Ca (mmol/L)	Ph (mmol/L)	UACR (mg/g)	HCO ₃ ⁻ (mmol/L)
<input type="text" value="Select..."/>	<input type="text"/>	<input type="text"/>	<input type="text"/>	<input type="text"/>	<input type="text"/>	<input type="text"/>

* You must fill in at least one of the six indicators. If there are multiple tests in a single month, please enter the average value of all tests for that month. Leave any missing test indicators blank.

Figure K.8: Website Snapshot: Manually Input. The figure demonstrates how to manually input patient data on the website.

KFDeep: a Deep Dynamic Kidney Failure Prediction Model

Instruction

```
graph TD; A[Choose DataUpload Method] --> B[Manual Entry]; A --> C[Upload Form]; B --> D[Fill as Required]; C --> E[Download Template]; E --> F[Fill as Required]; F --> G[Upload Data]; D --> H[Risk Assessment]; G --> H;
```

Data Upload

[Manual Entry](#) [Upload Form](#)

[Download Template](#) [Download Demo](#)

Instruction:

1. Please do not modify the headers of the file, only fill in the numbers.
2. In the first row of the "age" column, enter your age at the time of your first test.
3. In the first row of the "gender" column, enter your gender. Enter 2 if you are female and 1 if you are male.
4. Enter multiple test results. First, provide the test date in the "yyyymm" format (accurate to the month), followed by the corresponding test results for that date. The full names of the six indicators that need to be filled in are as follows: estimated glomerular filtration rate, urine albumin-to-creatinine ratio, albumin, blood calcium, blood phosphorus, and HCO3. You must fill in at least one of the six indicators. If there are multiple tests in a single month, please enter the average value of all tests for that month. Leave any missing test indicators blank.



Click to upload or drag the table into this area

Figure K.9: Website Snapshot: Upload Form. The figure illustrates how to fill out the template table and upload patient data using the table format. A demo file, demo.csv, is also provided on the page for demonstration purposes.

KFDeep: a Deep Dynamic Kidney Failure Prediction Model

The image shows a website interface for the KFDeep model. On the left, a flowchart titled "Instruction" outlines the process: "Choose DataUpload Method" leads to either "Manual Entry" or "Upload Form". "Manual Entry" leads to "Fill as Required", which then leads to "Risk Assessment". "Upload Form" leads to "Download Template", then "Fill as Required", then "Upload Data", and finally "Risk Assessment".

On the right, the "Data Upload" section is active. It has tabs for "Manual Entry" and "Upload Form". Below the tabs, there are links for "Download Template" and "Download Demo". A success message is displayed in a white box with a green checkmark: "After calculation, the probability value of kidney failure is 0.9034". Below the message is an "OK" button. The background shows a file upload area with a folder icon and the text "Click to upload or drag the table into this area". At the bottom left of the upload area, there is a file named "demo.csv".

Figure K.10: Website Snapshot: Output. The figure shows the website's output after uploading patient data from the demo.csv file.

The code for pytorch-free deployment:

```
import pandas as pd
import numpy as np

def sigmoid(x):
    return 1 / (1 + np.exp(-x))

def tanh(x):
    return np.tanh(x)

def calibration_value(value, percentiles=None):
    if percentiles is None:
        percentiles = [0, 1.302E-07, 2.514E-07, 5.142E-07, 1.178E-06,
            4.49407423123695E-06,
            0.000007568, 0.00001336, 0.00003832, 0.000226477, 1]
    for i in range(len(percentiles) - 1):
        if value <= percentiles[i + 1]:
            mapped_value = (value - percentiles[i]) / percentiles[i + 1] * 0.1
                + i * 0.1
            break
    return mapped_value

# model parameters
# The constant parameters W_d, b_d, W_i, b_i, W_f, U_f, b_f, W_g, U_g, b_g,
W_o, U_o, b_o, weight1, bias1, weight2, and bias2 can all be found on
GitHub at the following link: https://github.com/PKUDigitalHealth/KFDeep
.

W_d = [[0.28823587, ..., -0.40228388],
        ...,
        [-0.13478732, ..., 0.21852644]]
b_d = [3.0756582e-09, ..., 1.9038036e-02]
W_i = [[0.17907643, ..., -0.36906624],
        ...,
        [-0.25235277, ..., -0.2716872]]
U_i = [[0.15879741, ..., 0.07958254],
        ...,
        [-0.29005796, ..., 0.03001437]]
b_i = [1.32767131e-08, ..., -2.75927263e-08]
W_f = [[-0.45129496, ..., 0.00702733],
        ...,
        [-0.38420492, ..., 0.4881127]]
U_f = [[-0.381381, ..., 0.13979247],
        ...,
        [-0.3281368, ..., -0.1506905]]
b_f = [2.2645856e-09, ..., -1.1446243e-02]
```

```

W_g = [[-0.22903454, ..., -0.19572642],
        ...,
        [-0.06914535, ..., 0.3645177]]
U_g = [[-0.20168933, ..., 0.42868993],
        ...,
        [-0.03033528, ..., -0.04157215]]
b_g = [-1.2642247e-10, ..., -1.7966839e-10]
W_o = [[1.3190597e-01, ..., -3.0238628e-01],
        ...,
        [4.4741696e-01, ..., 5.1755682e-02]]
U_o = [[0.09416226, ..., -0.3430793],
        ...,
        [0.32326266, ..., -0.3349433]]
b_o = [1.6364738e-13, ..., -1.7292814e-05]
weight1 = [
    [-2.21271813e-01, ..., 6.26961291e-02],
    ...,
    [2.16766208e-01, ..., -2.18052283e-01]]
bias1 = [0.17824435, ..., 0.1561231]
weight2 = [[-0.18576701, ..., 0.02764091],
            [0.23119858, ..., -0.28893715]]
bias2 = [0.05485716, 0.31663576]

hidden_size = 16

if __name__ == '__main__':
    data = pd.read_csv('demo.csv')
    data = data.sort_values(by = 'date', ascending = True)
    data = data.groupby('date').agg(np.mean).reset_index()

    age = data['age'][0]
    gender = data['gender'][0]
    del data['age']
    del data['gender']

    interval_list = [0]
    for i in range(len(data) - 1):
        interval = int(str(data['date'][i + 1])[2:4]) * 12 + int(str(data['
            date'][i + 1])[4:6]) - \
            (int(str(data['date'][i])[2:4]) * 12 + int(str(data['date'][
                i])[4:6]))
        interval_list.append(interval)
    data['interval'] = interval_list
    del data['date']

    Cr = float(110) / 88.4

```

```

if gender == 2:
    eGFR = 144 * np.power(Cr / 0.7, -1.209) * np.power(0.993, age)
# for men
else:
    eGFR = 141 * np.power(Cr / 0.9, -1.209) * np.power(0.993, age)
missing_dict = {'egfr': eGFR,
                'albumin': 39,
                'ca': 2,
                'ph': 1,
                'uacr': float(np.exp(2.4738)),
                'hco3': 24.7}
data = data.interpolate()
data = data.bfill()
# if one for the variables are all none
for idx in missing_dict.keys():
    if pd.isnull(data[idx][0]):
        data[idx] = missing_dict[idx]

# transfer the type of input
data = data.values

# input data
x = data[:, :-1]
delta_t = data[:, -1]

# initialize parameters
h_t = np.zeros(hidden_size)
c_t = np.zeros(hidden_size)

# model
hidden_seq = []
seq_size = len(x)
for t in range(seq_size):
    x_t = x[t, :]
    delta_t_current = delta_t[t] + 0.1
    cs1_tb = np.tanh(c_t @ W_d + b_d)

    # Time decay function
    time_function = 1 / np.power(delta_t_current, 1)

    # T-LSTM Cell computation
    cs2_tb = cs1_tb * time_function
    c_t_b = c_t - cs1_tb
    cx_tb = c_t_b + cs2_tb

    # LSTM Gates computation

```

```

i_t = sigmoid(x_t @ W_i + h_t @ U_i + b_i)
f_t = sigmoid(x_t @ W_f + h_t @ U_f + b_f)
g_t = np.tanh(x_t @ W_g + h_t @ U_g + b_g)
o_t = sigmoid(x_t @ W_o + h_t @ U_o + b_o)

# Update cell state and hidden state
c_t = f_t * cx_tb + i_t * g_t
h_t = o_t * np.tanh(c_t)
hidden_seq.append(h_t)

time_output = weight1 @ h_t + bias1
mix_data = np.concatenate((time_output, [age, gender]))
outputs = weight2 @ mix_data + bias2
outputs = sigmoid(outputs)
pred = outputs[1] / (outputs[0] + outputs[1])
cal_pred = calibration_value(pred)
print(f"The risk is {cal_pred}")

```